Proceedings of the 2015 IEEE International Conference on Vehicular Electronics and Safety, Yokohama, Japan. Nov. 5-7, 2015.

A Model Predictive Combined Planning and Control Approach for Guidance of Automated Vehicles

Christian Götte*, Martin Keller*, Carsten Haß†, Karl-Heinz Glander†, Alois Seewald† and Torsten Bertram*
*Institute of Control Theory and Systems Engineering
TU Dortmund
44227 Dortmund, Germany
Email: Christian.Goette@TU-Dortmund.de
†ZF TRW
40547 Dusseldorf, Germany
Email: Carsten.Hass@TRW.com

***Abstract*—A novel approach for combined trajectory planning and control is presented in this contribution. The developed method integrates optimal control theory and trajectory planning and leads to an active safety system, which is applicable for automated driving and can avoid collisions in critical situations. The Combined Planning and Control (CPC) algorithm extends the Timed Elastic Band (TEB) approach by a suitable vehicle dynamics model, which facilitates stable vehicle guidance. The problem of trajectory generation is reformulated such that a nonlinear model predictive control (NMPC) method can be applied. The analysis of different traffic scenarios shows the functionality of the developed concept.**

I. Introduction

A major objective of automated driving is to generate a feasible trajectory regarding the constraints imposed by the vehicle environment and the prevalent physical laws. Automated vehicles have to be capable of handling normal driving strategies as well as emergency situations. The latter represents a challenging aspect of automated driving as the vehicle has to utilize its full dynamic capabilities. For emergency situations several path planning approaches have been presented using e.g. trapezoidal acceleration profiles [1] or sigmoidal functions [2]. A major drawback of these methods is that the planned path does not adapt to different traffic situations as it follows a predefined form. In [3] a different approach is introduced, which uses a propagation method to identify imminent and inevitable collisions in scenarios with multiple obstacles. By means of optimality criteria an evasive trajectory with minimal curvature is generated, feasible to perform a combination of braking and steering intervention. Another path planning approach is the concept of Elastic Bands that originates from mobile robot navigation and is introduced by [4]. Therein the initial path is modified reacting on local changes in the environment. This idea is transfered in terms of automotive applications for the generation of collision free trajectories in traffic scenarios [5], [6]. Both approaches enable evasive maneuvers using pure steering intervention, but neglect the possibility of braking to perform a combined steering and braking maneuver in emergency cases. The authors of [7] added a time component to the Elastic Band approach leading to the concept of a *Timed Elastic Band* (TEB), which enables the possibility to generate evasive trajectories with additional braking intervention. Based on the TEB an approach for critical traffic scenarios [8] and a similar approach for the purpose of autonomous driving [9] have been presented. These approaches consider kinodynamic constraints, but do not model nonlinear vehicle dynamics for cases of e.g. over- or understeer. A further drawback is that additional vehicle dynamics controllers have to be designed to realize the planned trajectory. For explicit consideration of vehicle stability and feasibility in the process of trajectory planning, knowledge of vehicle dynamics in form of a vehicle model is needed. The application of a vehicle model to perform trajectory generation is followed in the field of *nonlinear model predictive control* (NMPC), additionally negating the necessity of an underlying vehicle controller for trajectory following. In [10] a model predictive approach is presented for trajectory planning of combined steering and braking maneuvers. Tested on the scenario of pedestrian collision avoidance the authors consider nonlinear coupling effects in the vehicle dynamics. In [11] a single-track model is used for trajectory generation combined with a subordinated tracking controller and in [12] a NMPC approach using a double-track model for autonomous vehicle guidance is presented, utilizing an objective function that aims at tracking a state reference trajectory.

This paper focuses on a model predictive combined planning- and control approach for automated driving, which is also capable of handling critical situations. A collision free trajectory is planned considering vehicle dynamics, while generating the compatible control variables at the same time. The remainder of this paper is organized as follows. Section II gives a short overview on the used vehicle model. Section III describes the TEB approach as the basis of the work presented in this paper. Section IV presents the developed concept of a *Combined Planning and Control* (CPC) approach, integrating TEB theory and NMPC methods. The results are shown in Section V and in Section VI the paper is concluded.

II. Vehicle model

To capture the challenges of a critical situation the automated vehicle should be capable of performing an emergency maneuver. To utilize the vehicle's full dynamic capabilities steering and wheel independent braking have to be performed and considered in the process of trajectory planning and control. By wheel independent braking it is possible to generate additional torque around the vertical vehicle axis, also referred

to as yaw moment, which affects the lateral dynamics of the vehicle and enables the possibility to assist steering intervention. Another aspect which has to be considered concerning the choice of an appropriate prediction model is the model complexity, which represents a trade-off between accuracy and computational effort. Regarding the aforementioned requirements a simplified nonlinear double-track model is chosen to describe the vehicle dynamics.

Fig. 1 shows the applied nonlinear double-track model. Each of the four wheels of the vehicle is denoted with q, which is defined as

$$q = ij \qquad \begin{matrix} i = \{f, r\} : \text{front, rear} \\ j = \{l, r\} : \text{left, right} \end{matrix} .$$

The earth-, vehicle- and tire coordinate frame are used to describe the vehicle dynamics and denoted E, F and R respectively. The vehicle mass m and the moment of inertia around the vertical vehicle axis J_z are combined in the vehicle's center of gravity (CoG). The geometric parameters l_v, l_h, b_v and b_h describe the distances from the CoG to the front and rear axle and the front and rear track width respectively. The utilized double-track model is modeled with front steering, where the left and right front wheel can be turned by δ_r. Furthermore slip angle α, side slip angle β and yaw angle Ψ are depicted.

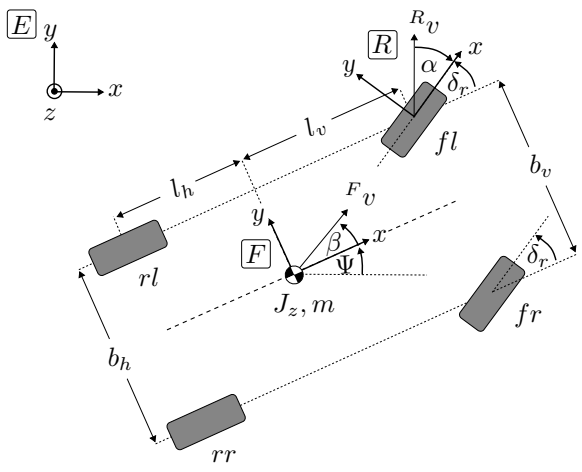

Fig. 1: Nonlinear double-track model.

A. Vehicle Dynamics

The double-track model can be represented as a nonlinear state-space model

$$\dot{\mathbf{x}}(t) = \mathbf{f}(\mathbf{x}(t), \mathbf{u}(t)), \quad \mathbf{x}(t_0) = \mathbf{x}_0 \tag{1}$$

with states $\mathbf{x}$

$$\mathbf{x} = \begin{bmatrix} {}^F v_x & {}^F v_y & {}^E\dot{\Psi} & {}^E\Psi & {}^E x & {}^E y \end{bmatrix}^T \tag{2}$$

and control variables $\mathbf{u}$

$$\mathbf{u} = \begin{bmatrix} \delta_l & s^{fl} & s^{fr} & s^{rl} & s^{rr} \end{bmatrix}^T . \tag{3}$$

The steering wheel angle δ_l can be expressed as a linear function of the wheel angle δ_r using the constant steering ratio i_s.

$$\delta_l = i_s \delta_r \tag{4}$$

Beside of the steering wheel angle δ_l the slip s^q at each wheel q of the vehicle is used as control input, assuming that the comparatively fast dynamics of the slip control system can be neglected.

B. Tire Model

The important value for determination of the tire forces in longitudinal direction is the slip s^q. The slip indicates the motion state of the tire and is defined as

$$s^q = \frac{r_{dyn}\ \omega - {}^R v_x^q}{\max\left(r_{dyn}\ \omega, {}^R v_x^q\right)} \tag{5}$$

with dynamic rolling radius r_{dyn} and the angular velocity ω. To determine the lateral tire forces the slip angle α^q is needed, which is defined as follows:

$$\alpha^q = -\arctan\left({}^R v_y^q / {}^R v_x^q\right). \tag{6}$$

An established and commonly used tire model is the magic tire formula [13]. Within CDC the magic tire formula is utilized, formulated such that the effects of combined slip are captured. Thus the applied tire model takes the coupled lateral and longitudinal force characteristics into account.

III. Timed Elastic Band

The TEB is a trajectory planning algorithm [7], [14]. It contains a set of vehicle configurations X as a sequence of n consecutive vehicle states $\mathbf{x}$ at each point in time t_k:

$$X := \{\mathbf{x}_k\}_{k=0\ldots n}\ , \qquad n \in \mathbb{N}. \tag{7}$$

The control input $\mathbf{u}_k$ is represented by the set U:

$$U := \{\mathbf{u}_k\}_{k=0\ldots n-1}\ , \qquad n \in \mathbb{N}. \tag{8}$$

The relevant physical values for describing the vehicle dynamics are consolidated in set Q, representing the tuple of the set of control variables U and the set of vehicle states X:

$$Q := (X, U)\,. \tag{9}$$

Vehicle states and control variables are extended by time intervals ΔT_k between two consecutive configurations so that a sequence

$$\tau := \{\Delta T_k\}_{k=0\ldots n-1} \tag{10}$$

of $n-1$ time differences is generated. Every time difference describes the available time for the transition from one configuration to the next. The TEB is defined as the tuple

$$B := (Q, \tau)\,. \tag{11}$$

For prediction horizon T and under consideration of given start values this leads to $n+1$ configurations of the TEB, which can be interpreted as band points. The objective is a weighted optimization of the TEB by minimizing a cost function $f(B)$, which combines l different objectives of an automated maneuver

$$f(B) = {}^1\!/_2 \cdot \mathbf{\Gamma}^T(B)\ \mathbf{\Gamma}(B), \quad \mathbf{\Gamma}(B) = \begin{bmatrix} \gamma_1 \mathbf{\Gamma}_1(B) \\ \gamma_2 \mathbf{\Gamma}_2(B) \\ \vdots \\ \gamma_l \mathbf{\Gamma}_l(B) \end{bmatrix}. \tag{12}$$

IV. Combined Planning and Control

For optimal trajectory generation with CPC the nonlinear double-track model is integrated into the TEB framework to ensure that feasible trajectories are produced. Time differences ΔT_k between two consecutive band points are assumed to be constant, because time optimality seems not to be a general goal of an optimal trajectory, regarding for example emergency collision avoidance maneuvers. By integration of system dynamics into the TEB framework the problem of optimizing the TEB is reformulated as an optimal control problem. Planning and control of the trajectory are performed together within one single step.

A. Nonlinear Model Predictive Planning and Control

In general numerical approaches are used to solve nonlinear optimal control problems. In this paper the direct multiple shooting method as described in [15] is used for repeatedly solving the optimal control problem. Following the idea of direct multiple shooting the control variables are discretized similar to the definition of the TEB control variables in (8)

$$\mathbf{u}(t) = \tilde{\mathbf{u}}_k, \quad t \in [t_k, t_{k+1}]. \tag{13}$$

In addition a discrete state vector $\tilde{\mathbf{x}}$ is introduced

$$\tilde{\mathbf{x}} = \begin{bmatrix} {}^{F}\tilde{v}_x & {}^{F}\tilde{v}_y & {}^{E}\tilde{\dot{\Psi}} & {}^{E}\tilde{\Psi} & {}^{E}\tilde{x} & {}^{E}\tilde{y} \end{bmatrix}^T. \tag{14}$$

The parameterized state trajectory is appended to the optimization variables and the vehicle state-space model (1) is solved in every interval independently from the other subintervals, starting with the initial value $\tilde{\mathbf{x}}_k$ of the state vector $\tilde{\mathbf{x}}$

$$\dot{\mathbf{x}}_k(t) = \mathbf{f}(\mathbf{x}_k(t), \tilde{\mathbf{u}}_k), \tag{15a}$$
$$\mathbf{x}_k(t_k) = \tilde{\mathbf{x}}_k. \tag{15b}$$

By integrating the state-space model in the subintervals $[t_k, t_{k+1}]$ the state trajectory $\mathbf{x}_k(t; \tilde{\mathbf{x}}_k; \tilde{\mathbf{u}}_k)$ is determined in dependency of the initial values $\tilde{\mathbf{x}}_k$ and control variables $\tilde{\mathbf{u}}_k$

$$\mathbf{x}_k(t_{k+1}; \tilde{\mathbf{x}}_k; \tilde{\mathbf{u}}_k) = \int_{t_k}^{t_{k+1}} \mathbf{f}(\tilde{\mathbf{x}}_k, \tilde{\mathbf{u}}_k)\ \mathrm{d}t. \tag{16}$$

The entire optimization problem is then given as:

$$\min_{\tilde{\mathbf{x}}, \tilde{\mathbf{u}}}\ f(B), \tag{17a}$$
$$\tilde{\mathbf{x}}_0 - \mathbf{x}_0 = 0, \tag{17b}$$
$$\tilde{\mathbf{x}}_{k+1} - \mathbf{x}_k(t_{k+1}; \tilde{\mathbf{x}}_k; \tilde{\mathbf{u}}_k) = 0, \tag{17c}$$
$$\mathbf{h}(\tilde{\mathbf{x}}_k, \tilde{\mathbf{u}}_k) = 0. \tag{17d}$$

The continuity constraint (17c) arises from the condition to satisfy the vehicle dynamics. This constraint is mandatory to obtain a valid solution for the optimal control variables $\tilde{\mathbf{u}}^*$. The trajectory constraints are considered by (17d). Furthermore no terminal constraints are imposed as in general there is no necessity of reaching a predefined terminal state. The constraints (17b)-(17d) are eliminated by substitution into the objective function $f(B)$ using the concept of softconstraints (24).

B. Objective Function

In the following a quantity at time t_k will be denoted with the leading subscript k. This is to emphasize the fact that the TEB is composed of several band points at time instances t_k with quantities of each band point being a part of the objective function. The continuity constraint (17c) of the optimization problem is integrated in the cost function and not formulated as a hard constraint, so that deviations between $\mathbf{x}$ and $\tilde{\mathbf{x}}$ are possible.

$${}_k\Gamma_{\Delta v_x}(B) = {}^{F}_{k}\tilde{v}_x - {}^{F}_{k}v_x, \tag{18}$$
$${}_k\Gamma_{\Delta v_y}(B) = {}^{F}_{k}\tilde{v}_y - {}^{F}_{k}v_y, \tag{19}$$
$${}_k\Gamma_{\Delta \dot{\Psi}}(B) = {}^{E}_{k}\tilde{\dot{\Psi}} - {}^{E}_{k}\dot{\Psi}, \tag{20}$$
$${}_k\Gamma_{\Delta \Psi}(B) = {}^{E}_{k}\tilde{\Psi} - {}^{E}_{k}\Psi, \tag{21}$$
$${}_k\Gamma_{\Delta x}(B) = {}^{E}_{k}\tilde{x} - {}^{E}_{k}x, \tag{22}$$
$${}_k\Gamma_{\Delta y}(B) = {}^{E}_{k}\tilde{y} - {}^{E}_{k}y. \tag{23}$$

Note that the deviations of $\mathbf{x}$ and $\tilde{\mathbf{x}}$ are squared during optimization process, when building the cost function (12). Considering numerical optimization the objective of a collision free trajectory is a challenging constraint. Therefore the hard constraint is reformulated as a piecewise continuous and differentiable softconstraint-function e_Γ, which penalizes the violation of a constraint:

$$e_\Gamma(z, z_e, \epsilon, n_e) \simeq \begin{cases} 0 & z \leq z_e - \epsilon \\ (z - (z_e - \epsilon))^{n_e} & z > z_e - \epsilon \end{cases} \tag{24}$$

with bound z_e, a small translation of the approximation ϵ and the polynomial order n_e. Position and velocity of the obstacle vehicles are supposed to be known from sensordata observing the environment. The extrapolated trajectories of the obstacle vehicles h are evaluated at discrete time instants, as they are assumed to move straight at a constant velocity. This yields

$${}^{E}_{k}x_h = {}^{E}_{k}x_{h,0} + {}^{E}_{k}v_{h,x} \cdot \Delta T_k, \tag{25a}$$
$${}^{E}_{k}y_h = {}^{E}_{k}y_{h,0} + {}^{E}_{k}v_{h,y} \cdot \Delta T_k \tag{25b}$$

and the euclidean distance between the trajectory of the ego vehicle and the obstacle vehicle at time t_k becomes

$${}_kd = \sqrt{\left({}^{E}_{k}x - {}^{E}_{k}x_h\right)^2 + \left({}^{E}_{k}y - {}^{E}_{k}y_h\right)^2}. \tag{26}$$

To model the rectangular shape of the vehicles, the minimal required distance d_{min} to avoid a collision is given by

$$d_{min} = d_1 + d_2 \cdot \cos^2(\Phi) \tag{27}$$

with Φ representing the relative orientation between the ego and the obstacle vehicle and parameters d_1 and d_2, which influence the form of the obstacle vehicle. Using (26) and (27) the constraint ${}_k\Gamma_{h,e_\Gamma}$ is

$${}_k\Gamma_{h,e_\Gamma}(B) = e_\Gamma(-{}_kd, -d_{min}, \epsilon_1, n_e), \tag{28}$$

describing the part of the objective function, which considers collision avoidance. To complete the environment modeling for all relevant aspects of automated driving in traffic scenarios the road limits are integrated in the cost function. This ensures that the vehicle stays on the road during the execution of the

planned maneuver. The constraint in form of the road limits is represented using the softconstraint-function e_Γ:

$$ {}_k\Gamma_{sl,e_\Gamma}(B) = e_\Gamma({}^E_k y, y_{max}, \epsilon_2, n_e), \tag{29} $$

$$ {}_k\Gamma_{sr,e_\Gamma}(B) = e_\Gamma(-{}^E_k y, -y_{min}, \epsilon_2, n_e). \tag{30} $$

By superposition of the costs from obstacle vehicles and road limits for each point in time t_k with $k = 0 \dots n$ an environment model is generated

$$ \mathbf{\Gamma_p}(B) = \mathbf{\Gamma_{h,e_\Gamma}}(B) + \mathbf{\Gamma_{sl,e_\Gamma}}(B) + \mathbf{\Gamma_{sr,e_\Gamma}}(B). \tag{31} $$

This environment model can be regarded as a potential field of the vehicle environment, which denotes negotiable areas. Fig. 2 illustrates an example of a resulting potential field, showing a scenario consisting of two lanes of 3.50 m width. During the maneuver both lanes can be used in positive x-direction. Road limits are imposed at $y_{min} = 1\,\text{m}$ and $y_{max} = 8\,\text{m}$ and an obstacle vehicle is positioned at the right lane 15 m ahead of the ego vehicle. This scenario is similar to the first test scenario investigated in section V. Beside the consideration of

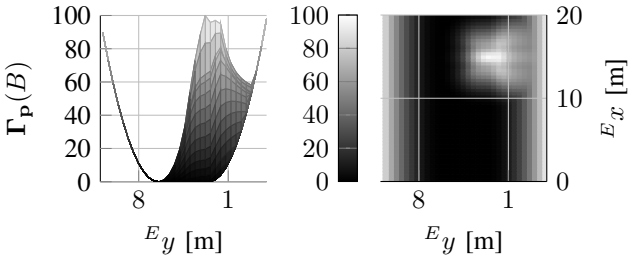

(a) Ego view (b) Top view

Fig. 2: Potential field of the ego vehicle environment.

constraints imposed by the environment of the ego vehicle, constraints on the control variables, taking the limited value range of the steering wheel angle and the slip at each wheel into account, are integrated in the cost function

$$ {}_k\Gamma_{\delta_l,e_\Gamma}(B) = e_\Gamma(|{}_k\delta_l|, \delta_{max}, \epsilon_3, n_e), \tag{32} $$

$$ {}_k\Gamma_{s^q_+,e_\Gamma}(B) = e_\Gamma({}_k s^q, s^q_{max}, \epsilon_4, n_e), \tag{33} $$

$$ {}_k\Gamma_{s^q_-,e_\Gamma}(B) = e_\Gamma(-{}_k s^q, -s^q_{min}, \epsilon_5, n_e). \tag{34} $$

The objective of generating an energy optimal trajectory is realized by penalizing the control variables. For a smooth behavior of the control input variables the derivatives are added to the cost function. For steering wheel angle δ_l this yields

$$ {}_k\Gamma_{\delta_l}(B) = |{}_k\delta_l|, \tag{35} $$

$$ {}_k\Gamma_{\dot\delta_l}(B) = |{}_k\dot\delta_l|, \tag{36} $$

$$ {}_k\Gamma_{\ddot\delta_l}(B) = |{}_k\ddot\delta_l| \tag{37} $$

and the penalties for slip s^q and its derivative are

$$ {}_k\Gamma_{\mathbf{s}^q}(B) = |{}_k s^q|, \tag{38} $$

$$ {}_k\Gamma_{\dot{\mathbf{s}}^q}(B) = |{}_k \dot s^q|. \tag{39} $$

To enable automated driving the ego vehicle is supposed to follow a reference speed ${}^F v_{ref}$, which is integrated in the cost function by

$$ {}_k\Gamma_v(B) = {}^F v_{ref} - {}^F v. \tag{40} $$

Further dynamic constraints are imposed by limiting side slip angle β

$$ {}_k\Gamma_{\beta,e_\Gamma}(B) = e_\Gamma(|{}_k\beta|, \beta_{max}, \epsilon_6, n_e) \tag{41} $$

as the value of β is used as an indicator for the stability of the performed maneuver.

Considering ${}_k\Gamma(B)$ for each point in time t_k with $k = 0 \dots n$ leads to a vector representation. Thus all different objectives for generating an optimal trajectory introduced as constraints and penalties can be combined, yielding

$$ \mathbf{\Gamma}(B) = \begin{bmatrix} \gamma_{\Delta\mathbf{v}_x} \cdot \mathbf{\Gamma}_{\Delta\mathbf{v}_x}(B) \\ \gamma_{\Delta\mathbf{v}_y} \cdot \mathbf{\Gamma}_{\Delta\mathbf{v}_y}(B) \\ \gamma_{\Delta\dot\Psi} \cdot \mathbf{\Gamma}_{\Delta\dot\Psi}(B) \\ \gamma_{\Delta\Psi} \cdot \mathbf{\Gamma}_{\Delta\Psi}(B) \\ \gamma_{\Delta\mathbf{x}} \cdot \mathbf{\Gamma}_{\Delta\mathbf{x}}(B) \\ \gamma_{\Delta\mathbf{y}} \cdot \mathbf{\Gamma}_{\Delta\mathbf{y}}(B) \\ \gamma_{\mathbf{h},e_\Gamma} \cdot \mathbf{\Gamma}_{\mathbf{h},e_\Gamma}(B) \\ \gamma_{\mathbf{sl},e_\Gamma} \cdot \mathbf{\Gamma}_{\mathbf{sl},e_\Gamma}(B) \\ \gamma_{\mathbf{sr},e_\Gamma} \cdot \mathbf{\Gamma}_{\mathbf{sr},e_\Gamma}(B) \\ \gamma_{\boldsymbol{\delta_l}} \cdot \mathbf{\Gamma}_{\boldsymbol{\delta_l}}(B) \\ \gamma_{\mathbf{s}^q} \cdot \mathbf{\Gamma}_{\mathbf{s}^q}(B) \\ \gamma_{\dot{\boldsymbol{\delta}}_l} \cdot \mathbf{\Gamma}_{\dot{\boldsymbol{\delta}}_l}(B) \\ \gamma_{\dot{\mathbf{s}}^q} \cdot \mathbf{\Gamma}_{\dot{\mathbf{s}}^q}(B) \\ \gamma_{\ddot{\boldsymbol{\delta}}_l} \cdot \mathbf{\Gamma}_{\ddot{\boldsymbol{\delta}}_l}(B) \\ \gamma_{\boldsymbol{\delta_l},e_\Gamma} \cdot \mathbf{\Gamma}_{\boldsymbol{\delta_l},e_\Gamma}(B) \\ \gamma_{\mathbf{s}^q_+,e_\Gamma} \cdot \mathbf{\Gamma}_{\mathbf{s}^q_+,e_\Gamma}(B) \\ \gamma_{\mathbf{s}^q_-,e_\Gamma} \cdot \mathbf{\Gamma}_{\mathbf{s}^q_-,e_\Gamma}(B) \\ \gamma_{\mathbf{v}} \cdot \mathbf{\Gamma}_{\mathbf{v}}(B) \\ \gamma_{\boldsymbol{\beta},e_\Gamma} \cdot \mathbf{\Gamma}_{\boldsymbol{\beta},e_\Gamma}(B) \end{bmatrix} \tag{42} $$

with weighting factors γ_l manually chosen to represent the priority of the respective objective. Building the cost function $f(B)$ using (12) leads to a nonlinear least-squares problem that can be solved by the *Levenberg-Marquardt Algorithm* (LMA). By dividing the optimization problem in subintervals a block-wise sparse Jacobian is generated, implying a sparse Hessian as well. The sparse structure can be used by the LMA to increase the computational efficiency of the algorithm.

V. Results

The performance of the proposed approach is evaluated in simulation studies. Therefore two test scenarios are chosen to illustrate the capabilities of CPC. In the first scenario a lane change maneuver is required to avoid the imminent collision with the static obstacle vehicle placed 40 m ahead of the ego vehicle at the center of the right lane. The first scenario is extended by another obstacle vehicle placed on the left lane at ${}^E x = 70\,\text{m}$, leading to a critical second test scenario. The ego vehicle moves with an initial velocity ${}^F v_0 = 100\,\text{km/h}$, which is also set to be the reference velocity ${}^F v_{ref}$.

A. Time Constants

The time distances of the TEB are $\Delta T = 0.1\,\text{s}$ with prediction horizon $T = 2\,\text{s}$, leading to a band with 21 band points. The integration step width for integrating the differential equations of the nonlinear double-track model using the explicit Euler method is $\Delta t = 0.01\,\text{s}$, which has shown to be sufficient concerning the prediction accuracy.

B. Simulation Results

A time series of the resulting trajectory in the first test scenario is depicted in Fig. 3, showing the ego vehicle in gray and the static obstacle vehicle in black. The corresponding

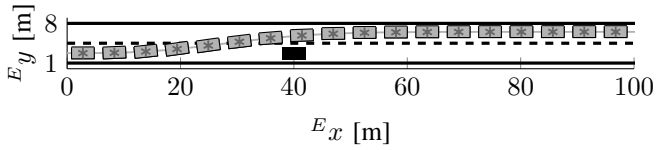

Fig. 3: Optimal trajectory of CPC (first test scenario).

optimal control variables to realize the maneuver are shown in Fig. 4. The steering wheel angle behaves as expected to realize a lane change. No braking intervention is applied so that the performed maneuver consists of sole steering. The

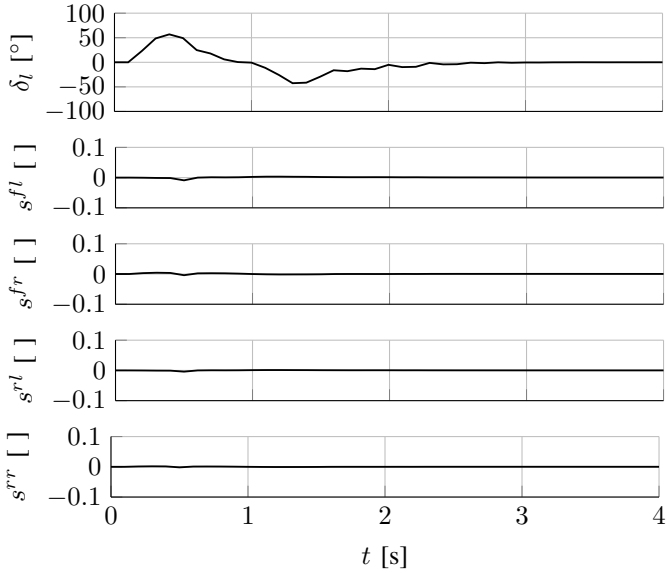

Fig. 4: Optimal control input $\tilde{\mathbf{u}}^*$ (first test scenario).

dynamic quantities of the maneuver are illustrated in Fig. 5. Longitudinal and lateral acceleration represent the course of a sole steering maneuver, so that as a consequence the velocity stays at constant $^F v = 100\,\text{km/h}$. The results of the first test scenario show that CPC performs well in less critical situations. Braking intervention is not applied regarding the aspect of energy optimality and the objective of following a predefined reference speed, while at the same time the objective of obstacle avoidance is satisfied. The resulting trajectory of CPC in the second test scenario is shown in Fig. 6. Right after the beginning of the maneuver all wheels of the vehicle are decelerated to reduce the speed. This is intended to avoid the imminent collision. After swerving around the obstacle vehicles the ego vehicle is accelerated to reach the reference speed $^F v_{ref}$ (see Fig. 7). For collision avoidance a compromise between longitudinal and lateral acceleration with respect to the physical limits has to be found. The performed maneuver in the critical second test scenario demands high lateral acceleration, but acceleration limits are not violated

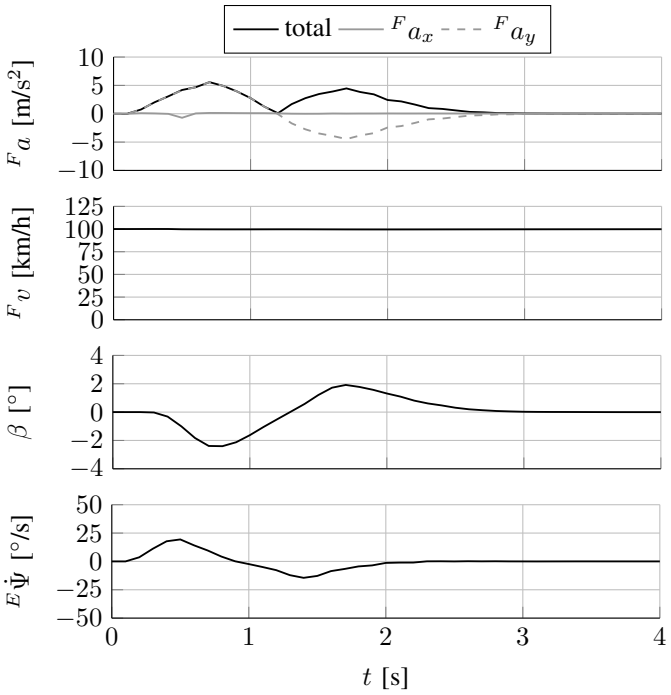

Fig. 5: Dynamic quantities (first test scenario).

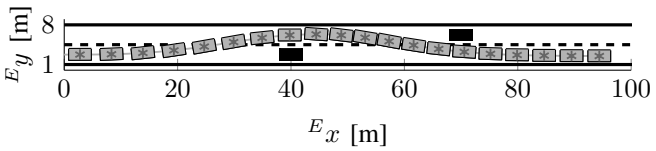

Fig. 6: Optimal trajectory of CPC (second test scenario).

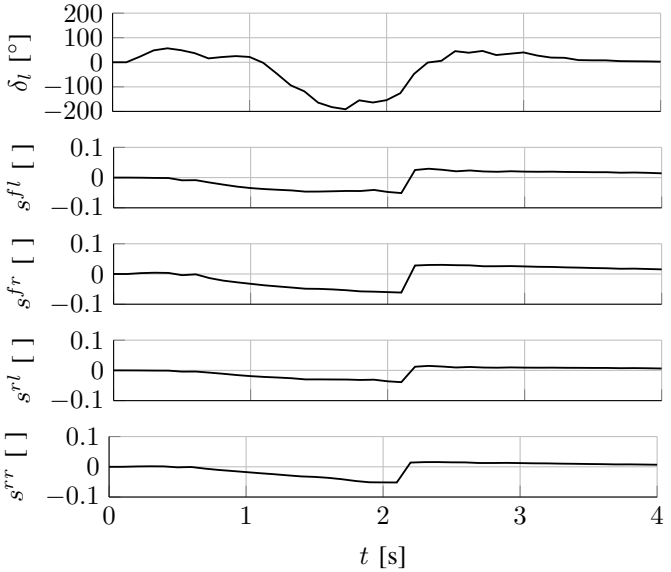

Fig. 7: Optimal control input $\tilde{\mathbf{u}}^*$ (second test scenario).

during the maneuver, as they are less than $^F a_{max} = 10\,\text{m/s}^2$. The illustrated results of the second test scenario motivate

the use of a nonlinear vehicle dynamics model, because by reaching the limits of driving physics in this critical situation it enables CPC to generate a trajectory, which still represents a valid solution. The depicted velocity shows the deceleration of the vehicle caused by the braking intervention, as well as the acceleration of the ego vehicle in the further course to reach the reference speed. Side slip angle β is small over the course of time. In combination with the depicted yaw rate it can be stated that the performed maneuver is stable (see Fig. 8).

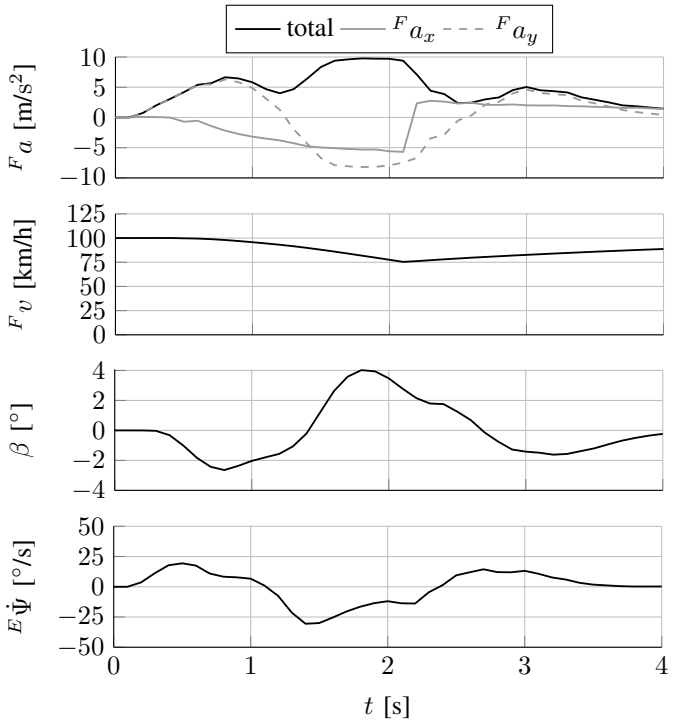

Fig. 8: Dynamic quantities (second test scenario).

VI. Conclusion

This contribution introduces a method for automated driving capable of handling critical traffic situations by combining optimal control theory and trajectory planning. Hence the developed CPC approach is capable of solving the problems of trajectory planning and vehicle control in one step. A nonlinear double-track model is integrated into the *Timed Elastic Band* approach, yielding an optimal control problem. This is efficiently solved by using the concept of softconstraints and direct multiple shooting as a state-of-the-art simultaneous nonlinear model predictive control method. The integration of a vehicle model enables the possibility to precisely formulate the restrictions in the objective function and ensures the generation of feasible control input variables implying the generation of a feasible trajectory. The chosen approach generalizes the aspect of vehicle guidance as the CPC algorithm is applicable to complex scenarios and not limited to a predefined situation. Information about the environment is sufficient to perform lateral and longitudinal vehicle guidance, including the decision whether to conduct a sole steering or a combined braking and steering maneuver. The aforementioned aspects are unique features of the CPC in contrast to other approaches. The analysis of the CPC generated maneuvers shows that collisions with the obstacle vehicles are avoided with respect to vehicle stability and physical limits. The computational costs of the presented algorithm are comparatively high, but on the other hand CPC is a very powerful method for trajectory planning and control. There are real-time implementations of NMPC problems with less optimization variables and as NMPC is a vital field of research with good improvements over the last years, further improvements can be expected. In addition the available computational power is supposed to increase. Further work will focus on improvements of the computational costs and studies on optimization issues such as the composition of the objective function and the choice of weighting factors.

References

[1] J. Choi, K. Yi, J. Suh, and B. Ko, "Coordinated control of motor-driven power steering torque overlay and differential braking for emergency driving support," *IEEE Transactions on Vehicular Technology*, vol. 63, no. 2, pp. 566–579, 2014.

[2] M. Schorn, U. Stahlin, A. Khanafer, and R. Isermann, "Nonlinear trajectory following control for automatic steering of a collision avoiding vehicle," in *Proceedings of the 2006 American Control Conference*, 2006, pp. 5837–5842.

[3] C. Schmidt, F. Oechsle, and W. Branz, "Research on trajectory planning in emergency situations with multiple objects," in *Proceedings of the IEEE Intelligent Transportation Systems Conference 2006*, 2006, pp. 988–992.

[4] S. Quinlan and O. Khatib, "Elastic bands: connecting path planning and control," in *IEEE International Conference on Robotics and Automation*, 1993, pp. 802–807.

[5] J. Hilgert, K. Hirsch, T. Bertram, and M. Hiller, "Emergency path planning for autonomous vehicles using elastic band theory," in *IEEE/ASME International Conference on Advanced Intelligent Mechatronics (AIM 2003)*, 2003, pp. 1390–1395.

[6] T. Sattel and T. Brandt, "Ground vehicle guidance along collision-free trajectories using elastic bands," in *Proceedings of the 2005 American Control Conference*, 2005, pp. 4991–4996.

[7] C. Rösmann, W. Feiten, T. Woesch, F. Hoffmann, and T. Bertram, "Trajectory modification considering dynamic constraints of autonomous robots," in *Proceedings of ROBOTIK 2012 - 7th German Conference on Robotics*, 2012, pp. 74–79.

[8] M. Keller, F. Hoffmann, T. Bertram, C. Haß, and A. Seewald, "Planning of optimal collision avoidance trajectories with timed elastic bands," in *Proceedings of the 19th IFAC World Congress*, 2014, pp. 9822–9827.

[9] J. Ziegler, P. Bender, T. Dang, and C. Stiller, "Trajectory planning for bertha — a local, continuous method," in *IEEE Intelligent Vehicles Symposium (IV), 2014*, 2014, pp. 450–457.

[10] M. Werling and D. Liccardo, "Automatic collision avoidance using model-predictive online optimization," in *IEEE 51st Conference on Decision and Control (CDC), 2012*, 2012, pp. 6309–6314.

[11] E. Bauer, F. Lotz, M. Pfromm, M. Schreier, B. Abendroth, S. Cieler, A. Eckert, A. Hohm, S. Lüke, P. Rieth, V. Willert, and J. Adamy, "Proreta 3: An integrated approach to collision avoidance and vehicle automation," *at - Automatisierungstechnik*, vol. 60, no. 12, pp. 755–765, 2012.

[12] J. V. Frasch, A. Gray, M. Zanon, H. J. Ferreau, S. Sager, F. Borrelli, and M. Diehl, "An auto-generated nonlinear mpc algorithm for real-time obstacle avoidance of ground vehicles," in *European Control Conference (ECC), 2013*, 2013, pp. 4136–4141.

[13] H. B. Pacejka, *Tyre and vehicle dynamics*, 2nd ed. Oxford: Butterworth-Heinemann, 2007.

[14] C. Rösmann, F. Hoffmann, and T. Bertram, "Timed-elastic-bands for time-optimal point-to-point nonlinear model predictive control," in *14th European Control Conference (ECC)*, 2015, pp. 3357–3362.

[15] M. Diehl, H. G. Bock, H. Diedam, and P.-B. Wieber, "Fast direct multiple shooting algorithms for optimal robot control," in *Fast Motions in Biomechanics and Robotics*. Heidelberg: Springer Berlin Heidelberg, 2005, vol. 340, pp. 65–93.